

InSARFlow: A high-performance program for time series InSAR processing and analysis of land deformation

Phong V.V. Le^a, Luyen K. Bui^b, Hai V. Pham^c, Anh N. Tran^a, Giang Nguyen-Van^d, Chien V. Pham^d, Phuong A. Tran^e

^a*Faculty of Hydrology Meteorology and Oceanography, VNU University of Science, Vietnam National University, Hanoi, Vietnam*

^b*Department of Spatial Sciences, Curtin University, Perth, WA, Australia*

^c*Division of Hydrologic Sciences, Desert Research Institute, Las Vegas, NV 89119, USA*

^d*Faculty of Water Resources Engineering, Thuyloi University, Hanoi, Vietnam*

^e*Water Research Institute, Hanoi, Vietnam*

Abstract

InSARFlow is a highly scalable, parallel software tool for land deformation and subsidence modeling. The program integrates **ISCE** and **GIA**nT software on a high-performance parallel framework for processing large-scale networks of interferograms and time series InSAR analysis. Its parallel computing engine is based on the distributed memory architecture using MPI. Written in Python, **InSARFlow** provides an easy-to-use platform for InSAR processing on high-end parallel supercomputers for the community.

Keywords: Land deformation, InSAR, parallel computing, python

Nr.	Code metadata description	Please fill in this column
C1	Current code version	v1.0
C2	Permanent link to code/repository used for this code version	https://github.com/levuvietphong/InSARFlow
C3	Code Ocean compute capsule	NA
C4	Legal Code License	GNU GPL v3.0
C5	Code versioning system used	git
C6	Software code languages, tools, and services used	Python 3.x
C7	Compilation requirements, operating environments & dependencies	Standard Python 3 installation
C8	If available Link to developer documentation/manual	https://github.com/levuvietphong/InSARFlow
C9	Support email for questions	levuvietphong@gmail.com

Table 1: Code metadata

1. Motivation and significance

Land subsidence, caused by the compaction of susceptible aquifer systems, is a significant global problem that affects many regions around the world [1–5]. Recently, time series interferometric synthetic aperture radar (InSAR) has offered a powerful tool for extracting the temporal evolution of surface deformation from a set of repeated SAR images [6–11]. With the launch of new SAR satellites (i.e. ALOS-2, Sentinel-1, etc), this radar remote sensing technique is capable of mapping a wide spatial coverage (~ 100 s km²) of land deformation with high vertical accuracy (~ 1 cm) and fine spatial resolution (~ 10 m or less) that is never possible before with techniques like GPS and leveling [12–14].

InSAR relies on the estimation of the phase difference or interferograms between complex-valued SAR images [15]. Error corrected and unwrapped interferograms are used to estimate land deformation rates using time series analysis algorithms, i.e. the persistent scatterer [16, 17] or distributed scatterer [18, 19] methods. For long-term subsidence detection, in order to limit temporal decorrelation, we must use many SAR images acquired at different times [20]. As a result, land subsidence modeling often requires processing a large number of interferograms.

The ever-increasing computing power of high-end parallel supercomputers is enabling the study of InSAR-based land deformation encompassing unprecedentedly large spatiotemporal scales. However, it also poses enormous algorithmic and computational challenges for scaling up the simula-

24 tions. In this paper, we present a high-performance, python-based software
 25 (**InSARFlow**) for land subsidence modeling. **InSARFlow** is unique in that it
 26 integrates InSAR Scientific Computing Environment (**ISCE**) [21] and Generic
 27 InSAR Analysis Toolbox (**GIAnt**) [22] toolboxes on a MPI-parallel structure
 28 for massive interferogram processing. This approach provides good scalabil-
 29 ity and acceleration of computation on parallel supercomputers. **InSARFlow**
 30 also facilitates data processing and transition from **ISCE** to **GIAnt**.

31 **2. Software description**

32 **InSARFlow** was designed to significantly reduce the amount of work and
 33 time to process SAR datasets and model land deformation. The software
 34 is written in Python due to its popularity and the availability of reliable
 35 packages (**ISCE** and **GIAnt**) for InSAR processing in the script language.
 36 **InSARFlow** offers parallel capabilities and additional helpful functions for
 37 InSAR time series processing.

38 *2.1. Software Architecture*

39 The implementation of **InSARFlow** is very simple that takes parameters
 40 from a single configuration file. The standard steps are: (i) download and
 41 process SAR images, (ii) construct a connected network among these images,
 42 (iii) calculate and unwrap interferograms in parallel, and (iv) post-process
 43 and perform time analysis for land deformation. Figure 1 shows the overview
 44 and main components of **InSARFlow**, including:

- 45 • **InSARFlowObjs.py**: provides classes to define and control model op-
 46 tions for different SAR data types.
- 47 • **InSARFlowFuncs.py**: contains key functions to download automati-
 48 cally SAR data, form an optimal connected network of images, and
 49 process a large number of interferograms in parallel using MPI.
- 50 • **InSARFlowGIAnt.py**: provides a tool to process **ISCE** outputs and run
 51 InSAR time series analysis in **GIAnt**.
- 52 • **InSARFlowTools.py**: provides tools for time series post-processing and
 53 visualization.

54 Currently, **InSARFlow** supports ALOS-PALSAR (L-band) and Sentinel-1
 55 (C-band) datasets that are global coverage and free available.

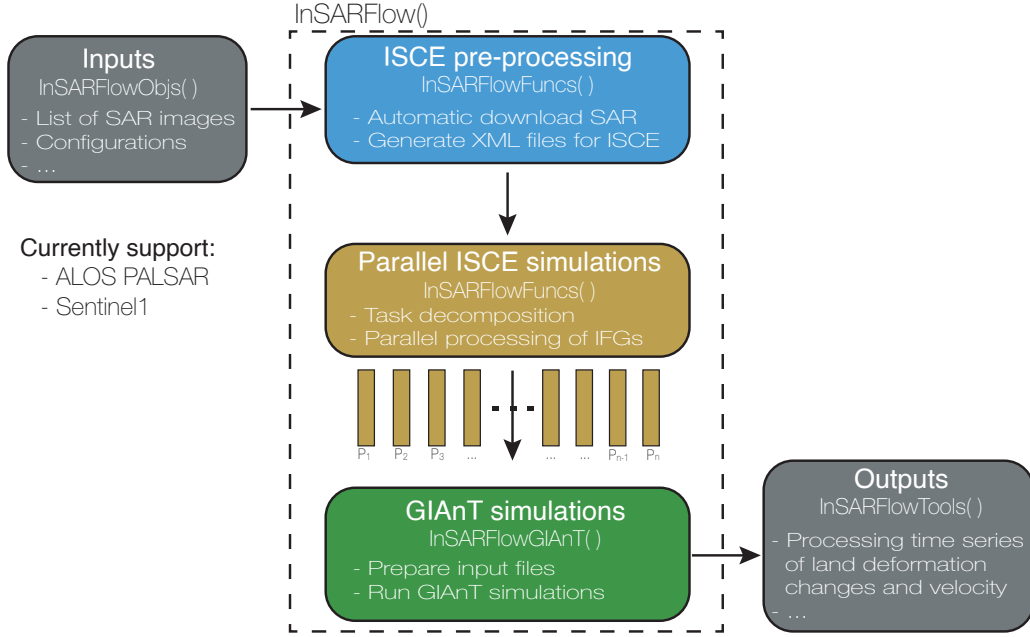


Figure 1: Overview of **InSARFlow** structure and functionality

56 2.2. Software Functionalities

57 There are three main functionalities of **InSARFlow**. First, it aims to as-
58 sist users to download and pre-process SAR images automatically. Given
59 the huge volume of datasets required for processing, these processes are of-
60 ten time-consuming and error-prone. All images are cropped to obtain a
61 common region before generating the interferograms. Second, **InSARFlow**
62 develops an optimal connected network of SAR images (see Figure 2) for
63 interferogram processing in parallel. Specifically, satellite images are consid-
64 ered as nodes, and the links among nodes are edges. Two nodes are linked
65 to each other if (i) their perpendicular baseline (the distance between two
66 acquisition spots) and temporal baseline (the time difference between two ac-
67 quisitions) are smaller than a given threshold and (ii) degree of connectivity
68 at each node is larger than a user-defined value. The network optimization
69 in **InSARFlow** is performed using **networkX** package. Finally, interferogram
70 processing is parallelized based on task decomposition using MPI. Because
71 the calculation of each interferogram is independent, running **ISCE** for many
72 interferogram can be implemented very efficiently in parallel. Figure 3 show
73 the strong-scaling test of **InSARFlow** as a function of computing nodes used.
74 The result show that time-to-resolution is reduced by a factor of 12.5 running
75 on 16 nodes compared to 1 node, representing descent scaling for **InSARFlow**
76 applications. The code is parallelized using **mpi4py** package.

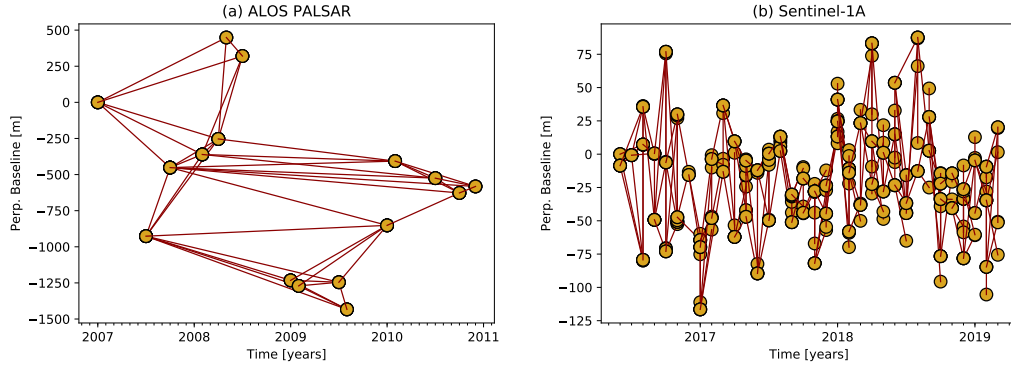


Figure 2: Network of interferograms for (a) 17 ALOS-PALSAR images from late 2006 to 2011 and (b) 81 Sentinel-1A images from mid 2016 to 2019. The x-axis show the time that images are acquired. The y-axis shows the perpendicular baseline with respect to the first image.

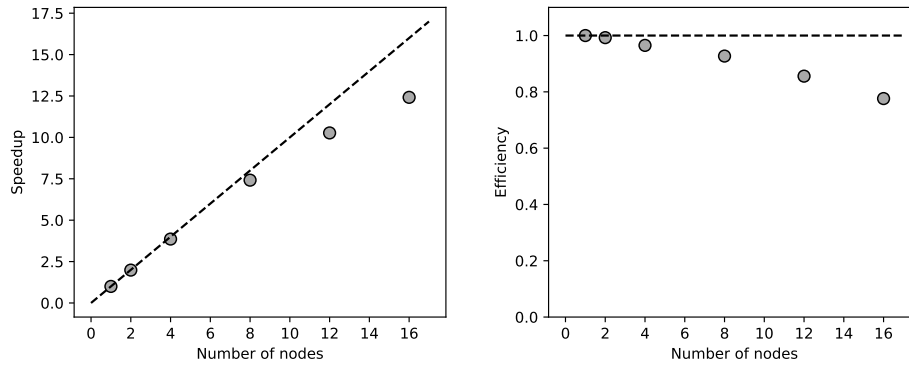


Figure 3: Strong scaling for speedup (left) and efficiency (right) of parallel code in InSARFlow. Dash line represents linear speedup (ideal) case.

77 3. Illustrative Examples

78 To demonstrate the performance of InSARFlow, two examples for land
 79 subsidence in the Mekong Delta using both ALOS-PALSAR and Sentinel-1A
 80 are provided along with the source code. In order to run InSARFlow, there
 81 are two mandatory files that must be presented in the correct structure: A
 82 configuration file (.cfg) showing all the options and a comma-separated values
 83 (.csv) file containing a list of SAR images for processing. Figure 4 shows two
 84 interferograms of the upper Mekong Delta using Sentinel-1A between several
 85 acquisition dates (Aug 27, 2017 and Oct 2, 2017; Nov 26, 2018 and Jan 25,
 86 2019).

Listing 1: Running ALOS-PASAR example in InSARFlow from command line

```
87 #!/bin/bash  
88 $ InSARFlow.py -c Mekong-ALOS.cfg
```

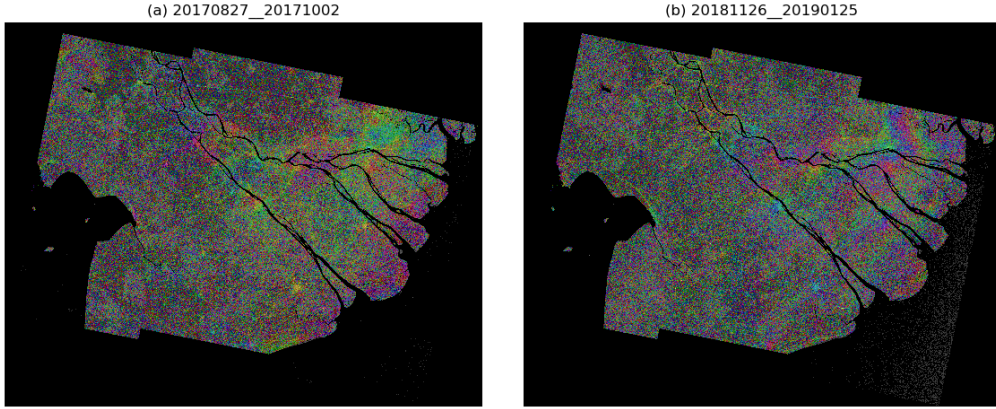


Figure 4: Examples of filtered and geocoded interferograms using Sentinel1-A in the Mekong Delta for (a) August 27, 2017 vs October 2, 2017 and (b) November 26, 2018 and January 25, 2019. In each interferogram, color represents phase difference between two SAR images used.

89 4. Impact

90 Two major impacts of the InSARFlow software are to: (i) facilitate land
91 deformation modeling by the integration of interferogram processing and
92 time series analysis into a single framework and (ii) provide an open-source,
93 scalable platform for large-scale InSAR processing on massively parallel su-
94 percomputers. New research questions can be pursued in the context of
95 high-performance computing for processing InSAR data.

96 5. Conclusions

97 InSARFlow is a high-performance and easy-to-use Python program for
98 land subsidence modeling. It contains a variety of functions for InSAR images
99 processing, network optimization, as well as being MPI-parallelized by the
100 task decomposition. It is designed to reduce the amount of work and time
101 to study large-scale land subsidence using both old and new SAR satellite
102 datasets. It has also been rigorously tested during multiple research projects
103 for different SAR images on machines of all sizes, from desktop to high-end
104 parallel computing platforms.

105 6. Conflict of Interest

106 The authors declared that they had no conflicts of interest with respect
107 to their authorship or the publication of this article.

108 Acknowledgements

109 This research is funded by Vietnam National Foundation for Science
110 and Technology Development (NAFOSTED) under grant number 105.06-
111 2017.320.

112 References

- 113 [1] H. Z. Abidin, R. Djaja, D. Darmawan, S. Hadi, A. Akbar, H. Rajiyowiry-
114 ono, Y. Sudibyo, I. Meilano, M. A. Kasuma, J. Kahar, C. Subarya, Land
115 subsidence of jakarta (indonesia) and its geodetic monitoring system,
116 Natural Hazards 23 (2) (2001) 365–387. doi:10.1023/A:1011144602064.
- 117 [2] J. Hoffmann, H. A. Zebker, D. L. Galloway, F. Amelung, Seasonal
118 subsidence and rebound in las vegas valley, nevada, observed by
119 synthetic aperture radar interferometry, Water Resources Research
120 37 (6) (2001) 1551–1566. doi:10.1029/2000WR900404.
121 URL [https://agupubs.onlinelibrary.wiley.com/doi/abs/10.](https://agupubs.onlinelibrary.wiley.com/doi/abs/10.1029/2000WR900404)
122 [1029/2000WR900404](https://agupubs.onlinelibrary.wiley.com/doi/abs/10.1029/2000WR900404)
- 123 [3] D. L. Galloway, T. J. Burbey, Review: Regional land subsidence accom-
124 panying groundwater extraction, Hydrogeology Journal 19 (8) (2011)
125 1459–1486. doi:10.1007/s10040-011-0775-5.
- 126 [4] S. A. Higgins, I. Overeem, M. S. Steckler, J. P. M. Syvitski, L. See-
127 ber, S. H. Akhter, Insar measurements of compaction and sub-
128 sidence in the ganges-brahmaputra delta, bangladesh, Journal of
129 Geophysical Research: Earth Surface 119 (8) (2014) 1768–1781.
130 doi:10.1002/2014JF003117.
131 URL [https://agupubs.onlinelibrary.wiley.com/doi/abs/10.](https://agupubs.onlinelibrary.wiley.com/doi/abs/10.1002/2014JF003117)
132 [1002/2014JF003117](https://agupubs.onlinelibrary.wiley.com/doi/abs/10.1002/2014JF003117)
- 133 [5] K. D. Murray, R. B. Lohman, Short-lived pause in central california
134 subsidence after heavy winter precipitation of 2017, Science Advances
135 4 (8). doi:10.1126/sciadv.aar8144.
136 URL <https://advances.sciencemag.org/content/4/8/eaar8144>

- [6] R. Bamler, P. Hartl, , Inverse Problems 14 (4) (1998) R1–R54.
doi:10.1088/0266-5611/14/4/001.
URL <https://doi.org/10.1088%2F0266-5611%2F14%2F4%2F001>
- [7] D. Massonnet, K. L. Feigl, Radar interferometry and its application to changes in the earth’s surface, Reviews of Geophysics 36 (4) (1998) 441–500. doi:10.1029/97RG03139.
URL <https://agupubs.onlinelibrary.wiley.com/doi/abs/10.1029/97RG03139>
- [8] P. A. Rosen, S. Hensley, I. R. Joughin, F. K. Li, S. N. Madsen, E. Rodriguez, R. M. Goldstein, Synthetic aperture radar interferometry, Proceedings of the IEEE 88 (3) (2000) 333–382. doi:10.1109/5.838084.
- [9] R. Bürgmann, P. A. Rosen, E. J. Fielding, Synthetic aperture radar interferometry to measure earth’s surface topography and its deformation, Annual Review of Earth and Planetary Sciences 28 (1) (2000) 169–209. doi:10.1146/annurev.earth.28.1.169.
- [10] A. Hooper, D. Bekaert, K. Spaans, M. Arıkan, Recent advances in sar interferometry time series analysis for measuring crustal deformation, Tectonophysics 514-517 (2012) 1 – 13. doi:<https://doi.org/10.1016/j.tecto.2011.10.013>.
- [11] Z. Yunjun, H. Fattahi, F. Amelung, Small baseline in-sar time series analysis: Unwrapping error correction and noise reduction, Computers & Geosciences 133 (2019) 104331. doi:<https://doi.org/10.1016/j.cageo.2019.104331>.
URL <http://www.sciencedirect.com/science/article/pii/S0098300419304194>
- [12] D. L. Galloway, K. W. Hudnut, S. E. Ingebritsen, S. P. Phillips, G. Peltzer, F. Rogez, P. A. Rosen, Detection of aquifer system compaction and land subsidence using interferometric synthetic aperture radar, antelope valley, mojave desert, california, Water Resources Research 34 (10) (1998) 2573–2585. doi:10.1029/98WR01285.
URL <https://agupubs.onlinelibrary.wiley.com/doi/abs/10.1029/98WR01285>
- [13] F. Amelung, D. L. Galloway, J. W. Bell, H. A. Zebker, R. J. Lacznia, Sensing the ups and downs of Las Vegas: InSAR reveals structural control of land subsidence and aquifer-system deformation, Geology 27 (6) (1999) 483–486. doi:10.1130/0091-7613(1999)027<0483:STUADO>2.3.CO;2.

- [14] M. Motagh, Y. Djamour, T. R. Walter, H.-U. Wetzels, J. Zschau, S. Arabi, Land subsidence in mashhad valley, northeast iran: results from insar, levelling and gps, *Geophysical Journal International* 168 (2) (2007) 518–526. doi:10.1111/j.1365-246X.2006.03246.x.
URL <https://onlinelibrary.wiley.com/doi/abs/10.1111/j.1365-246X.2006.03246.x>
- [15] A. K. Gabriel, R. M. Goldstein, H. A. Zebker, Mapping small elevation changes over large areas: Differential radar interferometry, *Journal of Geophysical Research: Solid Earth* 94 (B7) (1989) 9183–9191. doi:10.1029/JB094iB07p09183.
URL <https://agupubs.onlinelibrary.wiley.com/doi/abs/10.1029/JB094iB07p09183>
- [16] A. Ferretti, C. Prati, F. Rocca, Permanent scatterers in sar interferometry, *IEEE Transactions on Geoscience and Remote Sensing* 39 (1) (2001) 8–20. doi:10.1109/36.898661.
- [17] A. Hooper, H. Zebker, P. Segall, B. Kampes, A new method for measuring deformation on volcanoes and other natural terrains using insar persistent scatterers, *Geophysical Research Letters* 31 (23). doi:10.1029/2004GL021737.
URL <https://agupubs.onlinelibrary.wiley.com/doi/abs/10.1029/2004GL021737>
- [18] P. Berardino, G. Fornaro, R. Lanari, E. Sansosti, A new algorithm for surface deformation monitoring based on small baseline differential sar interferograms, *IEEE Transactions on Geoscience and Remote Sensing* 40 (11) (2002) 2375–2383. doi:10.1109/TGRS.2002.803792.
- [19] A. Ferretti, A. Fumagalli, F. Novali, C. Prati, F. Rocca, A. Rucci, A new algorithm for processing interferometric data-stacks: Squeesar, *IEEE Transactions on Geoscience and Remote Sensing* 49 (9) (2011) 3460–3470. doi:10.1109/TGRS.2011.2124465.
- [20] H. A. Zebker, J. Villasenor, Decorrelation in interferometric radar echoes, *IEEE Transactions on Geoscience and Remote Sensing* 30 (5) (1992) 950–959. doi:10.1109/36.175330.
- [21] P. A. Rosen, E. Gurrola, G. F. Sacco, H. Zebker, The insar scientific computing environment, in: *EUSAR 2012; 9th European Conference on Synthetic Aperture Radar*, 2012, pp. 730–733.

209 [22] P. S. Agram, R. Jolivet, B. Riel, Y. N. Lin, M. Simons,
210 E. Hetland, M.-P. Doin, C. Lasserre, New radar interfer-
211 ometric time series analysis toolbox released, Eos, Trans-
212 actions American Geophysical Union 94 (7) (2013) 69–70.
213 arXiv:<https://agupubs.onlinelibrary.wiley.com/doi/pdf/10.1002/2013EO070001>,
214 doi:10.1002/2013EO070001.
215 URL [https://agupubs.onlinelibrary.wiley.com/doi/abs/10.](https://agupubs.onlinelibrary.wiley.com/doi/abs/10.1002/2013EO070001)
216 [1002/2013EO070001](https://agupubs.onlinelibrary.wiley.com/doi/abs/10.1002/2013EO070001)